Influence of substrate compliance on buckling delamination of thin films

HONG-HUI YU and JOHN W. HUTCHINSON
Division of Engineering and Applied Sciences, Harvard University, Cambridge, MA 02138, U.S.A.

Abstract. A thin film subject to in-plane compressive stress is susceptible to buckling-driven delamination. This paper analyzes a straight-sided delamination buckle with a focus on the effects of substrate compliance, following earlier work by B. Cotterell and Z. Chen. The critical buckling condition, the energy release rate and the mode mix of the interface delamination crack are calculated as a function of the elastic mismatch between the film and substrate. The average energy release rate at the curved end of a tunneling straight-sided blister is also determined. The more compliant the substrate, the easier for the film to buckle and the higher the energy release rates. The effect becomes significant when the modulus of the substrate is appreciably less than that of the film. When the substrate modulus is comparable to that of the film, or higher, the usual assumption is justified to the effect that the film is clamped along its edges. When the substrate is very compliant the energy release rate at the curved front exceeds that along the straight sides.

Key words: Buckling, delamination, elastic mismatch, substrate compliance, thin films.

1. Introduction

Surface films and coatings often sustain substantial residual compressive stresses. This is especially true for ceramic coatings on metal substrates and metal films on polymer substrates if the temperature at deposition is higher than that at use. Examples are the oxide layer in a thermal barrier coating (e.g., Al_2O_3 on Ni-Cr-Al and Fe-Cr-Al alloys) (Tolpygo and Clarke, 1998) hard transparent coatings on optical polymers (Samson, 1996), and metal lines on polymer substrates in electronic packages. These surface layers are susceptible to buckling-driven delamination if the interface has low toughness. Various shapes of buckled region are observed, including long straight-sided blisters, circular and other equi-axed blisters, and the so-called 'telephone cord' blister. Apart from a recent study by Cotterell and Chen (2000), all of the analyses of thin film blisters have taken the films to be clamped around their boundaries, effectively regarding the substrate as rigid in the buckling analysis (e.g., Hutchinson and Suo, 1992; Gioia and Ortiz, 1997; Hutchinson et al., 1992; Nilsson and Giannakopoulos, 1995). Cotterell and Chen have shown that substrate compliance has an important influence on both the film buckling stress and the energy release rate of the interface delamination crack when the substrate modulus is appreciably smaller than that of the film. Their study was motivated by observations of buckling delamination of metal films on polymer substrates where the elastic mismatch is exceptionally large.

This paper gives the complete analysis of a straight-sided delamination buckle with focus on the role of substrate compliance. The present study confirms the findings of Cotterell and Chen (2000) and extends their results to arbitrary combinations of mismatch and blister size. In particular, a strong dependence of the substrate response to the ratio of blister size to film
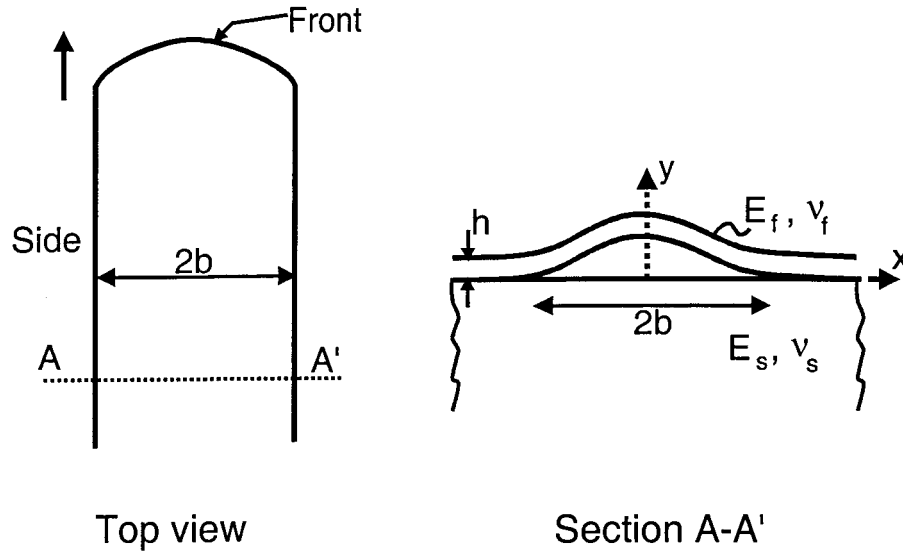
Figure 1. Geometry and notation for a straight-sided blister .The problem solved in the paper is the plane strain problem for a section $A' - A$ far behind the curved front. This solution is also used to generate the average energy release rate along the curved front for propagation under steady-state conditions.

thickness is revealed, which was not uncovered by Cotterell and Chen. These authors argued that the substrate response should be virtually independent of the blister width if the loads acting on it by the film are fixed, and they carried out calculations for one specific size to thickness ratio.

A characteristic length scale characterizing the film delamination problem will be identified which captures the essence of the role of the substrate compliance in the buckling delamination phenomenon. The next section of the paper presents the special film/substrate solution. The film buckling problem is coupled to the film/substrate solution in Section 3 providing the critical buckling condition along with the energy release rate and mode mix on the sides of the straight-sided blister (Figure 1). The energy release rate averaged over the curved front of the blister will also be given.

2. Film/substrate solution

A uniform and isotropic elastic film is bonded to an elastic substrate. A subscript '*f*' or '*s*', will be attached for reference to properties of the film and the substrate (Figure 1) such that E_f and v_f are the Young's modulus and Poisson's ratio of the film and E_s and v_s are the corresponding quantities for the substrate. The problem governing the behavior far behind the front of the straight-sided blister is a plane strain problem, and $\overline{E}$ is used to denote $E/(1-v^2)$.

The approach here is similar to that in Hutchinson and Suo (1992) and Cotterell and Chen (2000), in that the part of the film that is buckled is treated separately from the remaining film/substrate system. The behavior of the buckled portion of the film is modeled using von Karman nonlinear plate theory and is coupled to the film/substrate problem in Section 3. The film/substrate system (Figure 2) is a linear plane strain problem that is solved approximately using the integral equation formulation proposed by Yu et al. (2001) (Appendix). The solutions
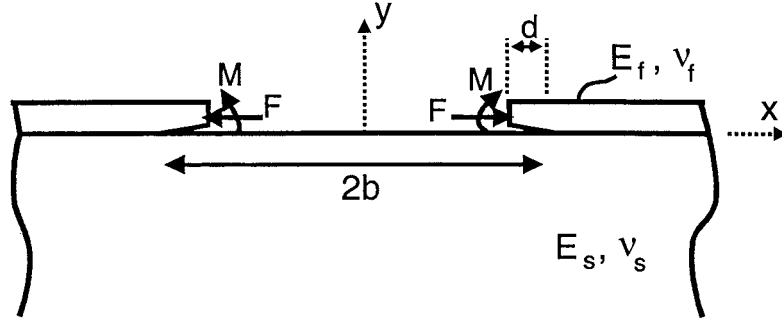
Figure 2. The plane strain problem for a film/substrate system with the buckled film removed.

of the two problems are matched at the detached edges of the film (with $d \to 0$) by requiring continuity of displacements and rotations.

As shown in Figure 2, h and b are the film thickness and blister half-width, respectively. A short segment of detached film of length d extends from each of the crack tips. The resultant force and moment per unit length acting on the film edges in Figure 2 are F and M, taken positive as shown. This problem is solved using the method described in Yu et al. (2001) (Appendix).

2.1. THE COMPLIANCE COEFFICIENTS, a_{ij}

Denote the effective horizontal displacement and rotation at the point $x = b$ where the film segment is attached to the substrate by $u|_{x=b}$ and $\theta|_{x=b}$, with θ positive for clockwise rotations. For any $d > h/4$, the horizontal displacement and rotation of the free end of the segment on the right ($b - d < x < b$) satisfy

$$
\begin{aligned}
u|_{x=b-d} - u|_{x=b} &= Fd/(\overline{E}_f h), \\
\theta|_{x=b-d} - \theta|_{x=b} &= 12Md/(\overline{E}_f h^3).
\end{aligned}
\tag{1}
$$

In other words, if $d > h/4$, the detached segment of can be treated as a plate that experiences uniform stretching and pure bending proportional to F and M, respectively, (Yu et al., 2001) with an effective displacement and rotation at the attachment point, $u|_{x=b}$ and $\theta|_{x=b}$. These relations define the effective displacement and rotation at the attachment point, and, by linearity,

$$
\begin{aligned}
u|_{x=b} &= a_{11}\frac{F}{\overline{E}_f} + a_{12}\frac{M}{\overline{E}_f h}, \\
\theta|_{x=b} &= a_{21}\frac{F}{\overline{E}_f h} + a_{22}\frac{M}{\overline{E}_f h^2},
\end{aligned}
\tag{2}
$$

with $a_{21} = a_{12}$. Defined in this manner, these quantities are independent of d. The coefficients a_{ij} are functions of both b/h and the Dundurs' elastic mismatch parameters, α and β, defined for plane strain problems as

$$
\alpha = (\overline{E}_f - \overline{E}_s)/(\overline{E}_f + \overline{E}_s),
$$

$$
\begin{aligned}
\beta = \tfrac{1}{2}[\overline{E}_f(1 - v_f)(1 - 2v_s) - \overline{E}_s(1 - v_s)(1 - 2v_f)]/[\overline{E}_f(1 - v_f)(1 - 2v_s) \\
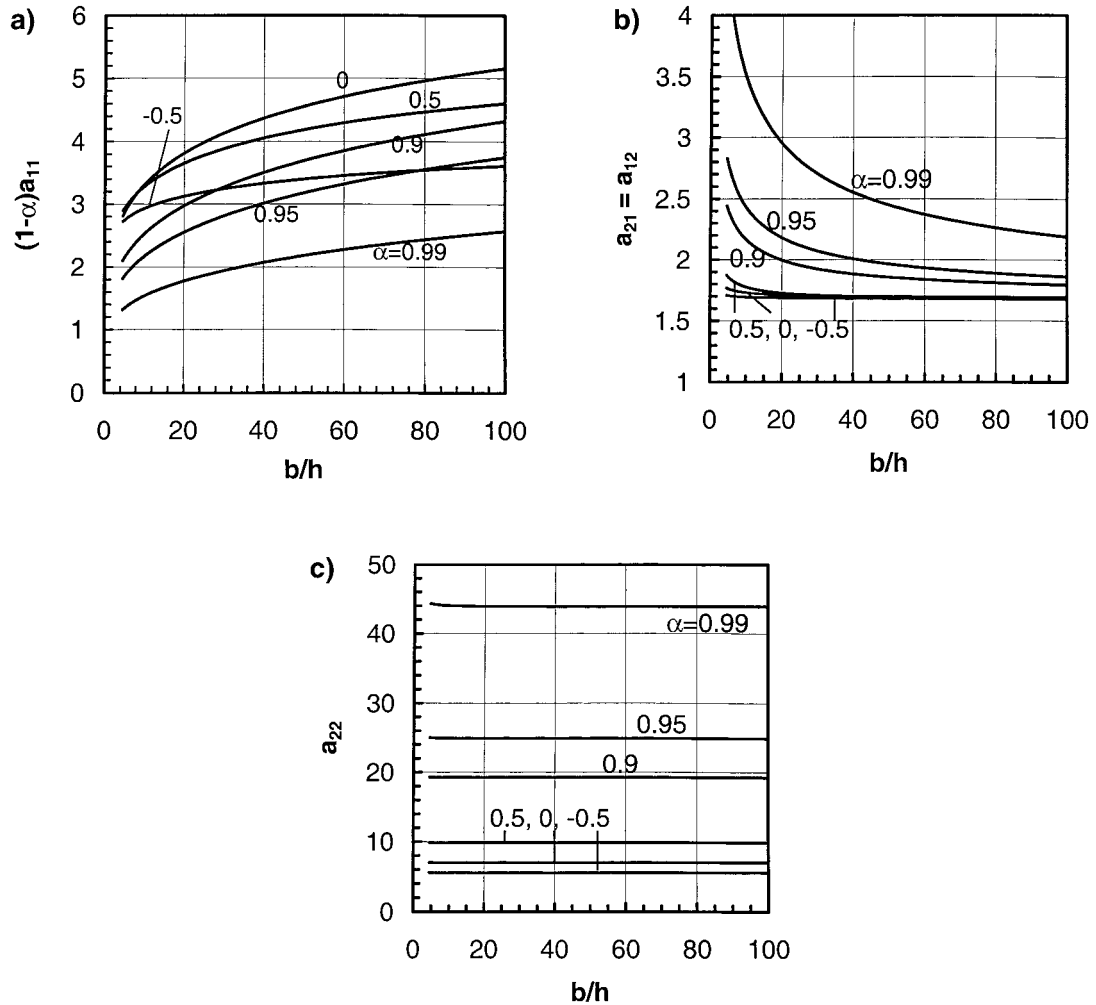+ \overline{E}_s(1 - v_s)(1 - 2v_f)].
\end{aligned}
\tag{3}
$$

Figure 3. The influence coefficients a_{ij} defined in (2) for the film/substrate problem.

Thus, $\alpha = -1$ when the substrate is rigid and α approaches 1 when the stiffness of the film to the substrate becomes large. The parameter β has a less important role than α in determining the coefficients a_{ij} in (2), as has been determined by selected calculations. Consequently, we shall concentrate on the role of α and take $\beta = 0$ in all the numerical results presented in the paper.

The coefficients a_{ij} are calculated by solving integral equations detailed in the Appendix. They are plotted in Figure 3 as a function of b/h for different values of α. While a_{22} is virtually independent of b/h, a_{11} and a_{12} have a strong dependence on both b/h and α. In fact, a_{11} increases in proportion to $\ln(b/h)$ for large b/h, as will be discussed shortly. A compliant substrate gives rise to a larger horizontal displacement, and a_{11} scales as $1/(1 - \alpha)$ when α is near unity. This scaling factor has been used in Figure 3a. The results obtained by Cotterell and Chen (2000) were restricted to $b/h = 100$. Our numerical results are in agreement with their results for this choice. In the next section, where the full coupled solution is presented, it will be apparent that the dependence of the a_{ij} on b/h is important.
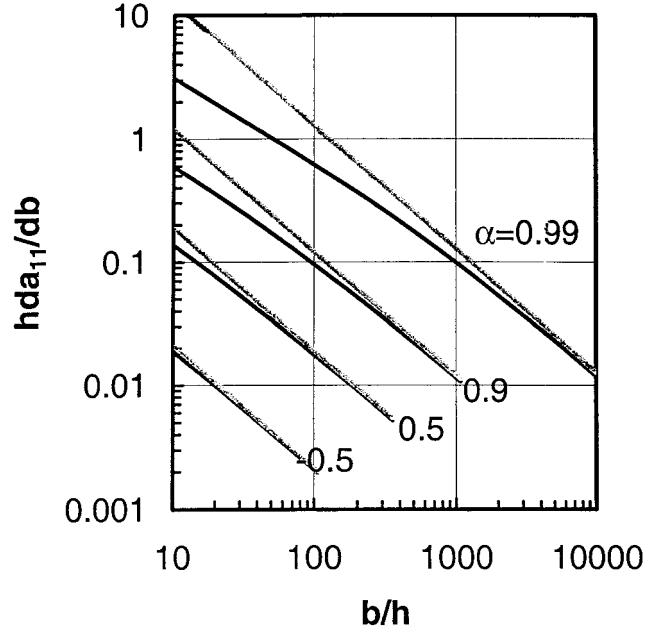
Figure 4. Comparison between the asymptotic result for $h\mathrm{d}a_{11}/\mathrm{d}b$ (dashed lines) with that from the full numerical analysis (solid lines) demonstrating the dependence of the influence coefficient on delamination width at large b/h.

When b/h is large enough, the strain at locations far away from the attachment points can be estimated by taking F and M as concentrated forces and moments applied at $x = \pm b$. Since the localized fields near the attachment points change negligibly when b/h further increases, the change of a_{11} can be readily estimated as:

$$\frac{\mathrm{d}a_{11}}{\mathrm{d}(b/h)} = \frac{2\overline{E}_f h}{\pi \overline{E}_s b}, \tag{4}$$

Verification that the asymptotic behavior of a_{11} is given by (4) when b/h is large can be seen in Figure 4, where (4) is compared with the full solution. When the film and substrate have comparable compliances, the asymptotic limit is approached at relatively small b/h. However, this approach is only attained at large b/h if the substrate is very compliant compared to the film.

2.2. THE STRESS INTENSITY COEFFICIENTS, c_{ij}

The stress intensity factors for the film/substrate problem in Figure 2 depend on F and M but they are independent of d for $d > h/4$. With $\beta = 0$, the factors for the tip at $x = b$ can be written as

$$K_{II} = c_{11}\frac{F}{\sqrt{h}} + c_{12}\frac{2\sqrt{3}M}{h\sqrt{h}}, \qquad K_I = c_{21}\frac{F}{\sqrt{h}} + c_{22}\frac{2\sqrt{3}M}{h\sqrt{h}}. \tag{5}$$

The dimensionless coefficients, c_{ij}, are determined in the solution process along with the a_{ij}. They also depend on b/h and α. When b/h is large these coefficients approach the limiting results of Suo and Hutchinson (1990), corresponding to the case where the two crack tips do not interact. The coefficients are plotted as a function of b/h for various a in Figure 5.
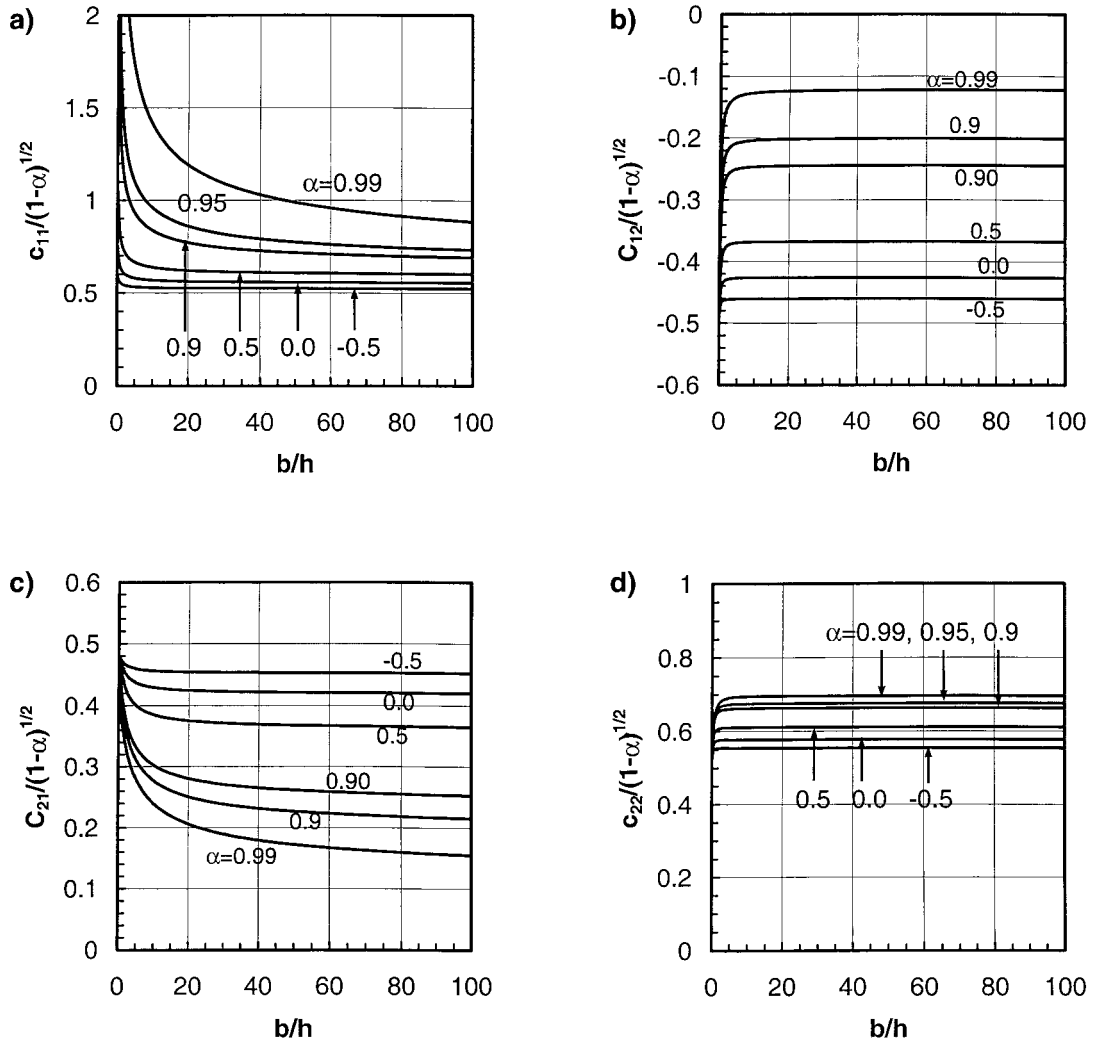
Figure 5. The coefficients c_{ij} in (5) defining the stress intensity factors in terms of the force and moment in the film at the edge of the delamination.

Because the c_{ij} scale as $\sqrt{1-\alpha}$ for $\alpha \rightarrow 1$ (see below), they have been normalized by this factor in the plots. The dependence of these coefficients on b/h is not nearly as strong as that of a_{ij}. Except for extremely compliant substrates, the Suo-Hutchinson limiting results should be sufficiently accurate for most relevant values of b/h. In that limit, $c_{21} = -c_{12}$.

The energy release rate of the interface crack in Figure 2 is related to the stress intensity factors by

$$G = \frac{(1-\beta^2)(K_I^2 + K_{II}^2)}{2} \left(\frac{1}{\overline{E}_f} + \frac{1}{\overline{E}_s} \right).$$
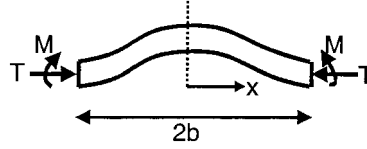
(6)

Figure 6. The detached buckled film.

2.3. A CHARACTERISTIC LENGTH, ℓ

A length ℓ can be derived that qualitatively characterizes the size of the zone of stress concentration near the points of attachment of the film in Figure 2. The length reflects the fact that the zone size is larger for compliant substrates than for stiff ones. To simplify the discussion, assume the film is subject to a loading with $F = \sigma h$. The resultant shear force in the K_{II}-dominant region along the interface must equilibrate F, to a first approximation, such that

$$\int_0^{\ell} \frac{K_{II}}{\sqrt{2\pi r}} \, \mathrm{d}r = q_1 \sigma h, \tag{7}$$

where q_1 is a number on the order of unity. Since the energy release rate G is on the order of $\sigma^2/(2\overline{E}_f)$ for this problem (exactly so as b/h becomes large), it follows from (6) that

$$K_{II} = q_2 \sigma \sqrt{\left(\frac{1-\alpha}{1-\beta^2}\right) h}, \tag{8}$$

where q_2 is related to the mode mix and is of order unity. Combining (7) and (8) and ignoring β, one can identify a compliance-dependent length as

$$\ell = \frac{2h}{(1-\alpha)} = \left(1 + \frac{\overline{E}_f}{\overline{E}_s}\right) h. \tag{9}$$

Interaction between the two crack tips is expected to be small when $b \gg \ell$, as borne out by the plots of the stress intensity coefficients in Figure 5. Similarly, validity of the asymptotic result for a_{11} in (4) also requires $b \gg \ell$, consistent with the results plotted in Figure 4.

3. Solution for buckled film coupled to the film/substrate system

Usually the film will be under a uniform, equi-biaxial compressive stress $\sigma_{\alpha\beta} = -\sigma \delta_{\alpha\beta}$ prior to buckling. However, an the results derived below are independent of the component of stress acting parallel to the straight edges of the blister. Thus, the important pre-stress component is $\sigma_{xx} \equiv -\sigma$. The delaminated film segment is modeled by von Kármán nonlinear plate theory. The vertical deflection and horizontal displacement of plate mid-surface are denoted by $w(x)$ and $u(x)$, respectively, both measured from the unbuckled state at stress σ. The theory is restricted to moderately large rotations, i.e., $[\mathrm{d}w/\mathrm{d}x]^2 \ll 1$. In the buckled state the ends of the delaminated segment of the film (Figure 6) are subject to a resultant compressive force per unit length, T, and a moment per unit length, M. By von Kármán plate theory, the horizontal resultant force throughout the buckled film is independent of x and therefore equal to T. The governing equation for the vertical deflection of the buckled film is

$$\frac{h^3 \overline{E}_f}{12} \frac{d^4 w}{dx^4} + T \frac{d^2 w}{dx^2} = 0, \tag{10}$$

The condition that T is x-independent requires that the horizontal displacement, u, satisfy

$$\frac{du}{dx} + \frac{1}{2} \left(\frac{dw}{dx} \right)^2 + \frac{T - \sigma h}{\overline{E}_f h} = 0. \tag{11}$$

The solution to (10) and (11), subject to symmetry about $x = 0$ with $u = u|_{x=b}$ and $dw/dx = -\theta|_{x=b}$ at $x = b$, provides the relations

$$u|_{x=b} = \frac{\sigma h - T}{\overline{E}_f} - \frac{\lambda h}{8} \left(\frac{M}{bT \ \cos \lambda} \right)^2 (2\kappa - \sin 2\lambda) \tag{12}$$

$$\theta|_{x=b} = -\frac{M\lambda}{Tb} \tan \lambda, \tag{13}$$

with $\lambda = \pi \sqrt{T/\sigma_* h}$. Here,

$$\sigma_* = \frac{\pi^2 \overline{E}_f}{12} \left(\frac{h}{b} \right)^2 \tag{14}$$

is the critical stress at the onset of buckling for a plate which is clamped on its edges, i.e., with $u|_{x=b} = 0$ and $\theta|_{x=b} = 0$. This critical stress serves as a reference against which to compare the critical stress when substrate compliance is taken into account.

The equations governing the dependence of M and T on σ, b and α are obtained by equating the expressions for the end displacement and rotation in (2) for the film/substrate system with those in (12) and (13) for the detached film. In doing so, one must identify F in (2) with $T - \sigma h$ because F is the *change* in resultant force per unit length measured relative to the pre-stressed state. One then obtains

$$(1 + a_{11}) \left(\frac{\sigma h - T}{\overline{E}_f h} \right) - \frac{\lambda(2\lambda - \sin 2\lambda)}{8} \left(\frac{M}{bT \ \cos \lambda} \right)^2 - a_{12} \frac{M}{\overline{E}_f h^2} = 0, \tag{15}$$

$$\frac{M}{bT} \lambda \ \tan \lambda + a_{22} \frac{M}{\overline{E}_f h^2} - a_{12} \left(\frac{\sigma h - T}{\overline{E}_f h} \right) = 0. \tag{16}$$

The bifurcation criterion giving the critical stress, σ_c, at the onset of buckling when the film first looses contact with the substrate is obtained by neglecting the term proportional to M^2 in (15) and then determining the eigenvalue equation from (15) and (16) as

$$\left[\frac{12b}{\pi h} \sqrt{\frac{\sigma_*}{\sigma_c}} \tan \left(\pi \sqrt{\frac{\sigma_c}{\sigma_*}} \right) + a_{22} \right] = \frac{a_{12}^2}{(1 + a_{11})}. \tag{17}$$

4. The effect of substrate compliance

In the following sub-sections, results will be presented for the effect of substrate compliance on: (1) the critical buckling condition, (2) the energy release rate and mode mix along the sides of the delamination blister, and (3) the energy release rate averaged over the curved

front of the blister. Delamination blisters are observed to propagate at the curved front, and the present results shed further light on this phenomenon for instances when the substrate modulus is very low compared to that of the film.

4.1. ONSET OF BUCKLING

To present results showing the influence of substrate compliance on the onset of buckling, it is useful to regard σ as prescribed and use (17) to compute the critical half -width, b_c, at which the film first deflects away from the substrate. For this purpose, define b_* to be the corresponding critical half width for the case where the film is clamped on its edges:

$$b_* = \frac{\pi h}{2\sqrt{3}}\sqrt{\frac{\overline{E}_f}{\sigma}}. \tag{18}$$

Thus, in (17), one can use

$$\frac{\sigma_c}{\sigma_*} = \left(\frac{b_c}{b_*}\right)^2 \tag{19}$$

such that (17) becomes

$$\left[2\sqrt{3}\sqrt{\frac{\overline{E}_f}{\sigma}}\tan\left(\pi\frac{b_c}{b_*}\right) + a_{22}\right] = \frac{a_{12}^2}{(1 + a_{11})}. \tag{20}$$

The a_{ij} given in Figure 3 depend on a and $b_c/h = (\pi/2\sqrt{3})\sqrt{\overline{E}_f/\sigma}\,(b_c/b_*)$.

   Curves of b_c/b_* as a function of the elastic mismatch parameter α computed from (20) are shown in Figure 7 for three representative values of $\sigma/\overline{E}_f$. The more compliant the substrate, the larger the reduction in the half width of the blister at the onset of buckling. Moreover, $\sigma/\overline{E}_f$ also has an effect on the result for a film that is clamped on its edges, i.e., $b_c/b_* \neq 1$ when $\alpha = -1$. This follows from the fact that the effective displacement and rotation of the film/substrate system in Figure 2 do not vanish in the limit of a rigid substrate. That is, the a_{ij} in (2) are non-zero for $\alpha = -1$ because the film allows for some deformation at the attachment point even though the substrate beneath it is rigid. Nevertheless, the difference between the critical half width for a film on the rigid substrate and that of a film fully clamped at its edges is quite small. In general, the reduction of the critical half width below that predicted for a fully clamped film only becomes significant when $\alpha > 1/2$, i.e., when $\overline{E}_f/\overline{E}_s > 3$.

4.2. ENERGY RELEASE RATE AND MODE MIX ALONG THE SIDES OF THE BLISTER

At $b > b_c$ or, equivalently, at $\sigma > \sigma_c$, the film buckles away from the substrate and one must solve (15) and (16) simultaneously for M and T. This is done numerically. Then, one uses (5) to compute the stress intensity factors along the sides of the blister, with F identified with $\sigma h - T$ as before. The energy release is computed from (6), and the measure of the mode mix is defined in the usual way as

$$\psi = \tan^{-1}(K_{II}/K_I). \tag{21}$$

Define the elastic energy per unit area in the unbuckled film that is available for release subject to plane strain (i.e., $\varepsilon_{zz} = 0$) as
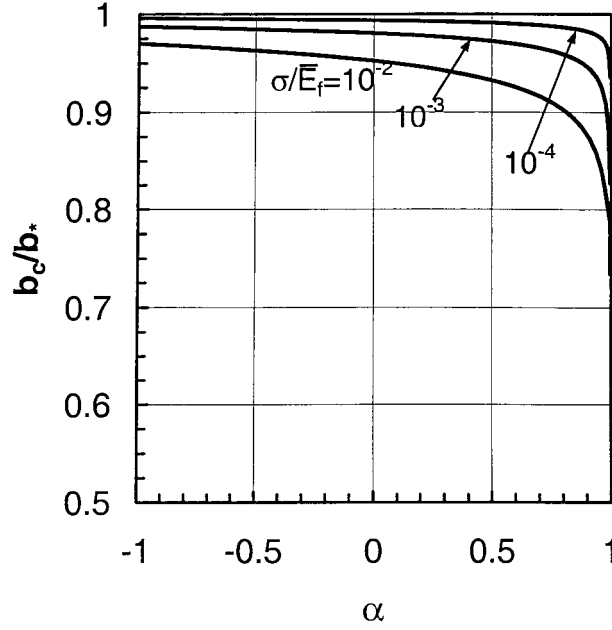
Figure 7. The roles of substrate compliance and pre-stress on the critical half width of the delamination, b_c, associated with the onset of buckling. The reference half width, b_*, is that for a film that is clamped along its edges (18).

$$G_0 = \frac{1}{2}\frac{\sigma^2 h}{\overline{E}_f}. \tag{22}$$

The computed results for G/G_0 as functions of b/b_* are shown in the four parts of Figure 8. Attention is first directed to the solid line curves which have been computed as described above; the dashed curves have been computed by a different scheme which will be described later in the next sub-section. The results depend on both the mismatch parameter, α, and the pre-stress ratio, $\sigma/\overline{E}_f$. In each of the four parts, the result from the analysis based on a fully clamped film is plotted as a curve of open circular points. That result is independent of $\sigma/\overline{E}_f$, as well as α, and is given by (e.g., Hutchinson and Suo, 1992)

$$\frac{G}{G_0} = \left(1 - \left(\frac{b_*}{b}\right)^2\right)\left(1 + 3\left(\frac{b_*}{b}\right)^2\right). \tag{23}$$

The curves in Figure 8a for the case of no elastic mismatch between the film and substrate ($\alpha = 0$) show that the simpler analysis based on the assumption of a clamped film is entirely adequate. Results for substrates that are stiffer than the films have not been shown since they are even more accurately approximated by (23). Even when the film modulus is three times the substrate modulus, as in Figure 8b, with $\alpha = 0.5$, the effect of the substrate compliance is not very large, although it elevates the peak value of the release rate by about 25% when $\sigma/\overline{E}_f = 0.01$. The effect of the substrate compliance becomes highly significant when $\alpha > 0.5$. Figures 8c, d display very large elevations in the peak energy release rate above (23) for $\alpha = 0.9$ ($\overline{E}_f/\overline{E}_s \cong 10$) and $\alpha \cong 0.99$ ($\overline{E}_f/\overline{E}_s = 100$), respectively. These elevations are comparable to those shown by Cotterell and Chen (2000) who, as already mentioned, based their computations on substrate responses fixed at $b/h = 100$.
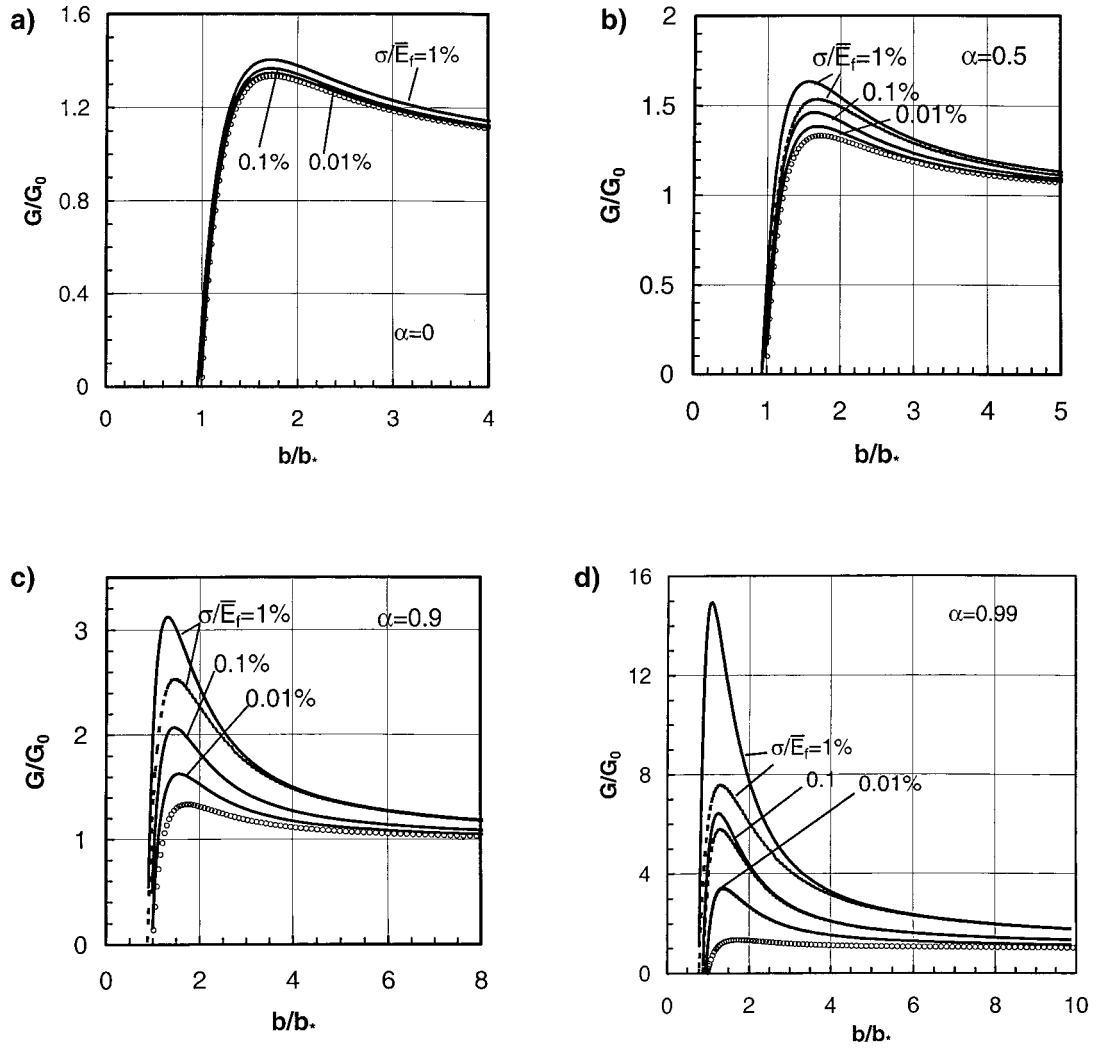
Figure 8. Normalized energy release rate along the sides of the delamination as a function of normalized blister width for several levels of pre-stress and for the elastic mismatches: (a) $\alpha = 0$; (b) $\alpha = 0.5$; (c) $\alpha = 0.9$; (d) $\alpha = 0.99$. The solid line curves have been computed using the expression for the energy release rate in terms of the stress intensity factors (6) with (5), while the dashed line curves are obtained using (24) with (25). The curve plotted as open circles is the prediction for a film clamped along its edge (23).

The physical basis of the higher energy release rates is due primarily to the release of elastic energy in regions of the film attached to the substrate as well as that from the delaminated portion of the film. When the substrate is compliant, the compressed film on the substrate along each edge of the delamination can deflect horizontally toward the center of the blister releasing part of its elastic energy. The more compliant the substrate, the wider will be the strip of film experiencing some relaxation and the greater will be the energy released. The width of this strip is proportional to the characteristic length, ℓ, introduced in (9). Thus, for very compliant substrates (e.g., $\overline{E}_f / \overline{E}_s \cong 100$), the width of the strips of film releasing extra elastic energy can be larger than the width of the buckled portion of the film. However, as b

increases, the relative contribution from the strips to the buckled portion diminishes, and, for sufficiently large b, G must still approach G_0.

The energy release rate can be computed in two ways: using (5) and (6) as was done above or by a more direct energy calculation based on

$$G = \frac{1}{2}\frac{\mathrm{d}\Delta U}{\mathrm{d}b}, \tag{24}$$

where ΔU is the total strain energy released per unit length of delamination. A direct evaluation of the difference between the elastic energy in the unbuckled and buckled states gives

$$\Delta U = \frac{(\sigma h)^2 b}{\overline{E}_f h} - \frac{T^2 b}{\overline{E}_f h} - 3\overline{E}_f h b \left(\frac{M}{\overline{E}_f h^2 \cos \lambda}\right)^2 (2 + \sin(2\lambda)/\lambda)$$
$$+ \frac{a_{11}}{\overline{E}_f}\left((\sigma h)^2 - T^2\right) - \frac{2a_{12}}{\overline{E}_f h}TM - \frac{a_{22}}{\overline{E}_f h^2}M^2. \tag{25a}$$

This expression can be reduced exactly to the following simpler expression with the aid of the governing equations (the steps of this reduction are omitted):

$$\Delta U = -(\sigma h - T)u|_{x=b} + \frac{(\sigma h - T)^2 b}{\overline{E}_f h}, \tag{25b}$$

where $u|_{x=b}$ is evaluated using (2) (again, with $F = T - \sigma h$).

If the theory governing the delamination problem and all the computations were exact, the two ways of evaluating G, by (6) with (5) or by (25), would necessarily give the same results. In fact, there are differences that appear when the substrate is very compliant and when the film stress is very high. The differences can be seen in Figure 8 where results computed using (24) and (25), which are shown as dashed line curves, can be compared with the results determined from the stress intensity factors. No differences are evident for $\alpha = 0$ and 0.5, and even for $\alpha = 0.9$ a difference only appears at the highest stress, $\sigma/\overline{E}_f = 0.01$. For the case of the most compliant substrate shown with $\alpha = 0.99$ a small difference appears when $\sigma/\overline{E}_f = 0.001$, but a fairly large difference is evident in the vicinity of the peak release rate when $\sigma/\overline{E}_f = 0.01$. There are two possible sources of this discrepancy. The analysis of the film/substrate problem given in the Appendix is not exact, but we believe it is highly accurate (Yu et al., 2001) and does not produce significant error in this regard. Moreover, linear elasticity is almost certainly valid for this problem. The second, and most likely, source is the fact that the governing theory pieces together a solution based on nonlinear plate theory with a solution to the linear film/substrate problem. The plate theory is only accurate as long as the rotations are only moderately large (i.e., $|\mathrm{d}w/\mathrm{d}x|^2 \ll 1$), and this condition is increasingly encroached upon as $\sigma/\overline{E}_f$ increases, especially when the substrate is very compliant.

The measure of the mode mix, ψ, associated with the interlace crack on the delamination sides is plotted in Figure 9 a function of b/b_*. The mode mix is fairly insensitive to $\sigma/\overline{E}_f$ and has almost the same dependence on the elastic mismatch as predicted by the simpler analysis of Hutchinson and Suo (1992) which takes the plate to be clamped on its edges. The important feature to note is the tendency for a higher proportion of mode I to mode II for blisters on more compliant substrates, an effect that will promote delamination for most systems.
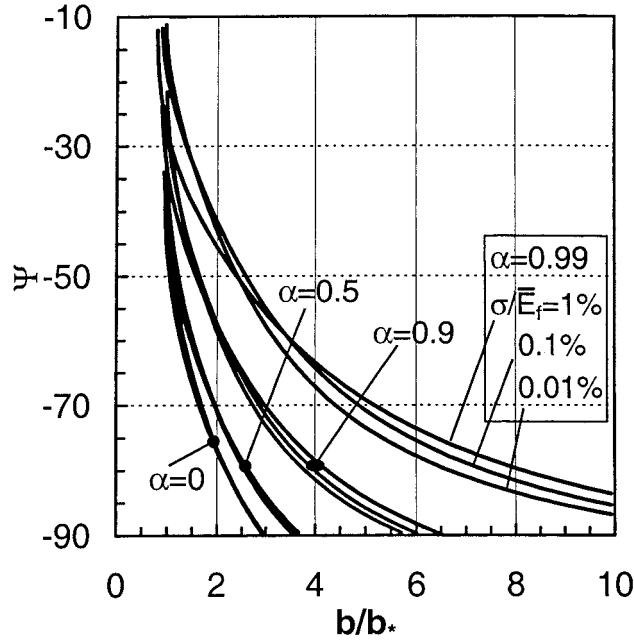
Figure 9. Mode mix along the sides of the delamination as a function of the normalized blister width, elastic mismatch, and pre-stress.

4.3. ENERGY RELEASE RATE ON THE CURVED FRONT OF A TUNNELING DELAMINATION

The total energy released per unit length of delamination, ΔU, is equal to the energy released by the delamination blister in advancing a unit of length under steady-state propagation at its curved front (cf., Figure 1). It follows immediately that the energy release rate averaged over the curved front is simply

$$G_{ss} = \frac{\Delta U}{2b}. \tag{26}$$

Curves of G_{ss}/G_0 versus b/b_* are plotted as solid lines in Figure 10 computed by (25) and (26). Included in each of the four plots are the curves from Figure 8 as determined from (5) and (6) for the energy release rate on the sides of the blister, G/G_0. As long as the film is not too stiff compared to the substrate, e.g., $\alpha < 0.5$, the steady-state release rate associated with the curved front is less than the release rate on the sides of the blister. The result for $\alpha = 0$ in Figure 10a is very close to the result of Hutchinson and Suo (1992) for the blister clamped on its edges, i.e.,

$$\frac{G_{ss}}{G_0} = \left(1 - \left(\frac{b_*}{b}\right)^2\right)^2. \tag{27}$$

These authors also found that the mode mix along the curve front has a much higher proportion of mode I to mode II than along the sides. It is this feature, along with the mode dependence of interface toughness, which is essential to the explanation of why such blisters propagate at the curved front and not on the sides.

An interesting new development occurs for films that are much stiffer than their substrates, i.e., $\alpha \geq 0.9$ in Figures 10c and 10d. As noted by Cotterell and Chen (2000), the steady state
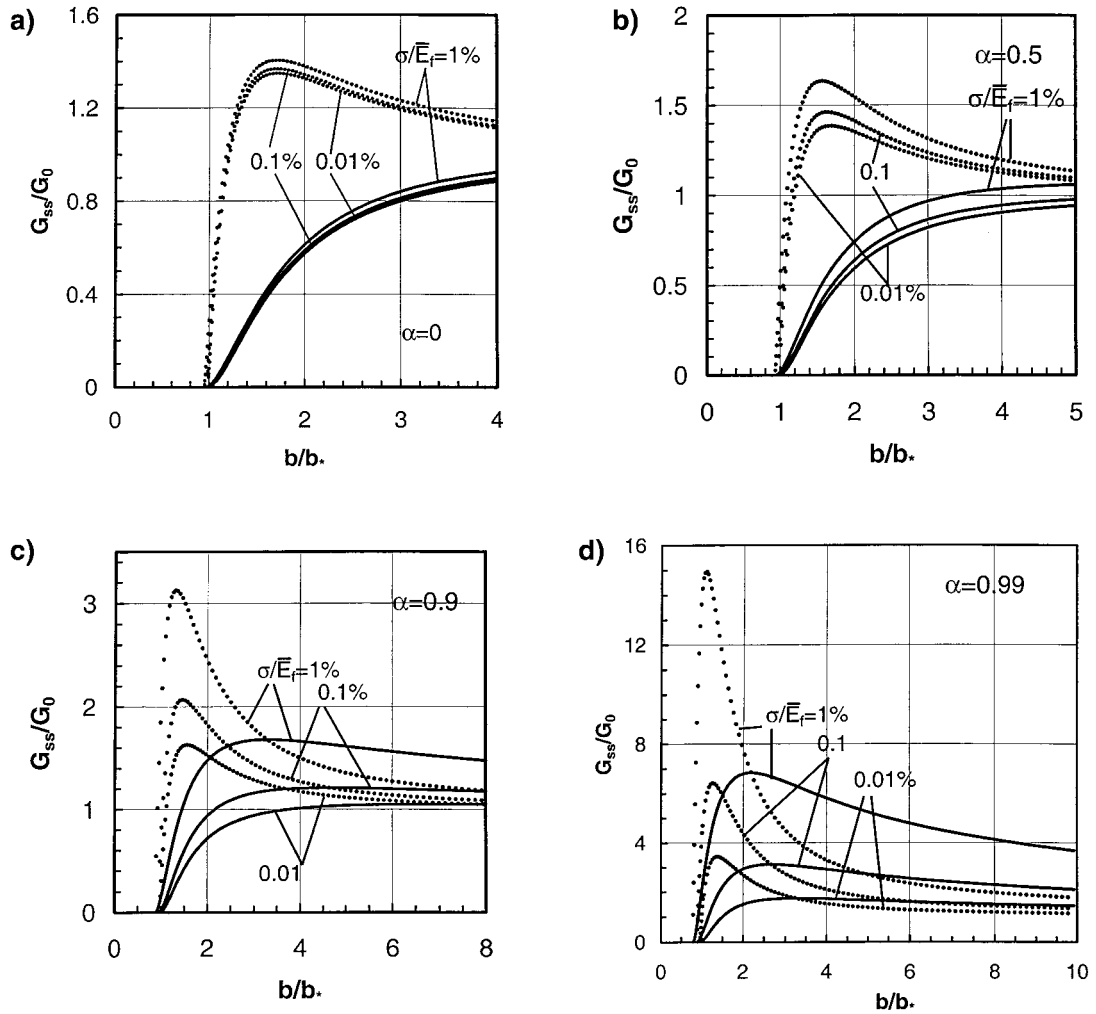
Figure 10. The normalized average energy release rate along the curved front of a steadily propagating straight-sided blister (solid lines) for the elastic mismatches: (a) $\alpha = 0$; (b) $\alpha = 0.5$; (c) $\alpha = 0.9$; (d) $\alpha = 0.99$. For comparison, the energy release rate along the sides of the delamination is also shown as dashed curves.

tunneling release rate can now exceed the energy release rates along the sides if the blister exceeds a certain width. The effect is significant for $\alpha = 0.99$. In principle, this means that, once formed, such a blister would propagate at its curved front even if the interface toughness were mode independent.

5. Conclusions

Substrate deformation has a significant effect on thin film buckling delamination when the ratio of the film modulus to substrate modulus exceeds about 3. The effects will be particularly pronounced for films and coatings of metals and ceramics on polymer substrates where the modulus ratio can be 100 or more. There is also likely to be important consequences for some systems having ceramic films on metal substrates such as alumina on aluminum or diamond on various metals. Buckling delamination of diamond films on silicon substrates is widely

observed and displays particularly dramatic morphologies. Diamond on silicon has a modulus ratio of about 10, corresponding to $\alpha \cong 0.9$. Substrate deformation is almost certainly an influential factor for this system, cf., Figures 8c and 10c.

The present analysis confirms the work of Cotterell and Chen (2000) who were the first to call attention to the importance of substrate deformation in this phenomenon. The present work has extended their analysis by demonstrating the strong dependence the substrate contribution on the ratio of blister size to film thickness as well as the elastic mismatch.

The essential aspect of the substrate deformation is partial release of elastic energy in the regions of the film still bonded to the substrate along the edges of the delamination. The width of this release zone scales with the characteristic length, $\ell = (1 + \overline{E}_f / \overline{E}_s)h$. Thus, the more compliant the substrate compared to the film, the more energy released from the film. The energy release rate for a delamination crack on an interface between a stiff film and a highly compliant substrate can be many times that for systems with comparable elastic moduli. The effect is not unlike the corresponding role of substrate compliance in the cracking of thin films in tension. In that phenomenon, a crack channeling through the film has an enhanced energy release rate if the substrate is compliant relative to the film, all other factors being equal (Beuth, 1992; Shenoy et al., 2000).

A qualitative change in behavior appears when the film modulus exceeds that of the substrate by a factor of about ten or more. Then the energy release rate along the curved front of the delamination blister becomes greater than that along the sides for sufficiently wide blisters. This would allow for the existence of propagating straight-sided blisters even if the interface toughness is mode independent. How substrate compliance affects other delamination shapes remains to be determined.

Finally, we remark again that one of the Dundurs parameters defined in (5), β, has been taken as zero in the results presented in the paper. However, selected calculations were also performed for the critical buckling width and the energy release rate using $\beta = \alpha/4$, which represents about as large a value of β as usually encountered. The differences between the energy release rates and those plotted in Figures 8 and 10 are inconsequential and have not been shown. The effect on the measure of mode mixity will also be small as can be seen from results given in Hutchinson and Suo (1992).

Acknowledgements

Appendix: Integral equations of interface tractions

Yu, He and Hutchinson (2001) proposed a new model for the analysis of thin film deformation. The reader is referred to that paper for background to the detailed expressions that follow for the film/substrate problem illustrated in Figure 2. The derivatives of the displacements on the right-hand interface with respect to x are expressed as functions of the tractions along the interface:

$$\mathrm{d}u/\mathrm{d}x = \frac{1-2\nu_f}{1-\nu_f}\frac{\sigma_{yy}(x)}{\overline{E}_f} - \frac{2}{\pi\overline{E}_f}\int_b^\infty \frac{\sigma_{xy}(\xi)}{\xi - x}\mathrm{d}\xi$$

$$+\frac{1}{2\pi\overline{E}_f}\int_b^\infty\left[4\frac{-\sin 2\omega - 2\omega}{h} + 6\frac{(1-\cos 2\omega)(x-\xi)}{h^2}\right]\sigma_{xy}(\xi)\,\mathrm{d}\xi, \quad \text{(A1a)}$$

$$+\frac{1}{2\pi\overline{E}_f}\int_b^\infty\left[4\frac{\cos 2\omega - 1}{h} - 6\frac{(\sin 2\omega - 2\omega)(x-\xi)}{h^2}\right]\sigma_{yy}(\xi)\,\mathrm{d}\xi$$

$$\mathrm{d}v/\mathrm{d}x = -\frac{1-2\nu_f}{1-\nu_f}\frac{\sigma_{xy}(x)}{\overline{E}_f} - \frac{2}{\pi\overline{E}_f}\int_b^\infty \frac{\sigma_{yy}(\xi)}{\xi - x}\mathrm{d}\xi + \int_b^x \frac{m}{\overline{E}_f I}\mathrm{d}x + \theta_0, \quad \text{(A1b)}$$

where

$$\omega = \arctan\frac{x-\xi}{h}, \quad \text{(A2)}$$

$$m(x) = M + \int_b^\infty [(1-\cos 2\omega)(x-\xi) - (\sin 2\omega + 2\omega)h/2]\frac{\sigma_{xy}(\xi)}{2\pi}\mathrm{d}\xi$$

$$- \int_b^\infty [(\sin 2\omega - 2\omega)(x-\xi) + (1-\cos 2\omega)h/2]\frac{\sigma_{yy}(\xi)}{2\pi}\mathrm{d}\xi, \quad \text{(A3)}$$

and θ_0 is a constant to be determined. Equations (A1a) and (A1b) were derived from solving elastic problem of thin film alone. The same derivatives of the displacement with respect to x, obtained from the elastic solution for the substrate, are:

$$\mathrm{d}u/\mathrm{d}x = \frac{1-2\nu_s}{1-\nu_s}\frac{\sigma_{yy}(x)}{\overline{E}_s} + \frac{2}{\pi\overline{E}_s}\int_b^\infty \frac{2\xi\sigma_{xy}(\xi)}{\xi^2 - x^2}\mathrm{d}\xi, \quad \text{(A4a)}$$

$$\mathrm{d}v/\mathrm{d}x = -\frac{1-2\nu_s}{1-\nu_s}\frac{\sigma_{xy}(x)}{\overline{E}_s} + \frac{2}{\pi\overline{E}_s}\int_b^\infty \frac{2x\sigma_{yy}(\xi)}{\xi^2 - x^2}\mathrm{d}\xi, \quad \text{(A4b)}$$

The symmetry of σ_{yy} and anti-symmetry of σ_{xy} with respect to $x = 0$ have been included in (A4). Two integral equations for the interface tractions are obtained by equating (A1) and (A4). The interface tractions should also satisfy the following equilibrium conditions:

$$\int_b^\infty \sigma_{xy}(\xi)\,\mathrm{d}\xi = -(\sigma h - T), \quad \text{(A5a)}$$

$$\int_b^\infty \sigma_{yy}(\xi)\,\mathrm{d}\xi = 0, \quad \text{(A5b)}$$

$$\int_b^\infty \sigma_{yy}(\xi)(\xi - b)\,\mathrm{d}\xi = -M - (\sigma h - T)h/2. \quad \text{(A5c)}$$

The integral equations are solved numerically using the scheme introduced in Erdogan et al. (1973).

References

Beuth, J.R. (1992). Cracking of thin bonded films in residual tension. *International Journal of Solids and Structures* **29**, 1657–1675.

Cotterell, B. and Chen, Z. (2000). Buckling and cracking of thin film on compliant substrates under compression, *International Journal of Fracture* **104**, 169–179.

Erdogan, F., Gupta, G.D. and Cook, T.S. (1973). Numerical solution of singular integral equations. In: *Methods of Analysis and Solutions of Crack Problems* (edited by Shih, G.C.), Noordhoff, Leiden, 368–425.

Gioia, G. and Ortiz, M. (1997). Delamination of compressed thin films. *Adv. Appl. Mech.* **33**, 120–192.

Hutchinson, J.W. and Suo, z. (1992). Mixed mode cracking in layered materials. *Advances in Applied Mechanics* **29**, 63–191.

Hutchinson, J.W., Thouless, M. And Liniger, E.G. (1992). Growth and configurational stability of circular, buckling-driven film delamination. *Acta Metall. Mater.* **40**, 295–308.

Nilsson, K.F. and Giannakopoulos, A.E.(1995). A finite element analysis of configurational stability and finite growth of buckling driven delaminations. *Journal of Mechanical and Physics of solids* **43**, 1983–2021.

Samson, F. (1996). Ophthalmic lens coating. *Surf. Coat. Tech.* **81**, 79–86.

Shenoy, V.B., Schwartzman, A.F. and Freund, L.B. (2000). Crack patterns in brittle thin films. *Int. J. Fracture* **103**, 1–17.

Suo, Z. and Hutchinson, J.W. (1990). Interface crack between two elastic layers. *International Journal of Fracture* **43**, 1–18.

Yu, H.H., He, M.Y. and Hutchinson, J.W. (2001). Edge effects in thin film delamination. *Acta Mater.* **49**, 93–107.